Liquid-vapor Partitioning of Aqueous Electrolytes

at Temperatures to the Solvent Critical Point[1]

J. M. Simonson,[2] Donald A. Palmer, and Miroslav S. Gruszkiewicz

Chemical and Analytical Sciences Division

Oak Ridge National Laboratory

P. O. Box 2008, Bldg. 4500S, MS-6110

Oak Ridge, TN 37831-6110 USA

---

[2] To whom correspondence should be addressed.

ABSTRACT

Measurements of the equilibrium partitioning of aqueous electrolytes between liquid and vapor give information which can be used to establish plausible speciation models for the solutes in both phases, as well as practical knowledge of the extent of solute transport in steam cycle applications. In a series of experimental and modeling studies, we have shown that for strong electrolytes (e.g., NaCl) the observed solute partitioning is consistent with the assumption of complete association of electrolytes to neutral species in low-density steam, with very modest ion association in the liquid phase even at relatively high concentrations. For weaker electrolytes (e.g., HCl) the degree of dissociation of the solute in the liquid phase at a given temperature and molality is lower, with higher measured volatilities of the solute. Under these speciation assumptions, values of the electrolyte association constant K_A at the critical temperature and density of the solvent, determined by measurements of electrical conductance or other methods, provide an independent check of the consistency of the volatility results and an "anchor point" for modeling the temperature and density dependencies of the distribution constant K_D. These phase-equilibrium measurements can also be used in some cases to give information on the activity coefficients of species in the liquid phase at high temperatures and concentrations. Examples of partitioning behavior in pure and mixed aqueous electrolyte solutions including HCl(aq) and {NaCl + HCl}(aq) illustrate the use of measured compositions of coexisting phases to give equilibrium distribution constants, information on liquid-phase activity coefficients, and indications of the extent of ionization of the solute in both the liquid and vapor phases.

KEY WORDS: activity coefficient; aqueous solutions; electrolytes; speciation; vapor-liquid equilibria; volatility

2

INTRODUCTION

The volatility of electrolyte solutes in aqueous solution, or equivalently, the partitioning of electrolytes between liquid water and saturated steam, is an important consideration in a number of natural and technological systems even though the vapor-phase electrolyte concentration is very small under most subcritical conditions. For example, corrosion of system materials and deposition of solids have been found in the steam cycles of central power plants even under relatively stringent guidelines for impurity limits in the water used in the cycle. In geothermal power systems based on either the flashing of steam from concentrated brines or the production of "dry" steam from underpressured (steam-dominated) reservoirs, the partitioning of electrolytes between liquid and steam can lead to rapid corrosion of well and piping systems and in extreme cases force particular wells to be shut-in and abandoned. Measurements of the volatility of aqueous electrolytes is also of fundamental interest, in that the partitioning of solutes between phases can be interpreted in terms of the extent of association of the solutes to neutral species in each phase.

The importance of the technological problem of impurity transport in power plant steam cycles is evident from the long history of investigations in this area. An early summary report by Straub [1] includes a number of references dating back to the 1930's. At that time it was considered that "soluble" compounds were transported through liquid droplets, and that the carryover of these (primarily electrolyte) components through steam was negligible. As temperatures increased in Rankine-cycle plants in an effort to improve cycle efficiency and better methods were used to reduce the amount of entrained liquid droplets in steam, transport of dissolved solids in steam

became an increasingly important source term for deposition and corrosion processes. A number of investigations of the solubility of salts in supercritical steam and of the liquid-vapor phase equilibria of "nonvolatile" (e.g., electrolyte) solutes at subcritical temperatures, were carried out in the former Soviet Union, and particularly by Styrikovich and coworkers [2-8]. These studies led to the widespread use of the "ray diagram" describing the partitioning of solutes between liquid and steam as a simple function of the ratio of the densities of the phases. A primary motivation for the work at ORNL described here was the observation by Jonas and others [9] that the ray diagram did not accurately represent the observed carryover of solutes in operating fossil-fired power plants.

In the following sections the apparatus and techniques used to determine the compositions of coexisting liquid and vapor phases at high temperature are briefly reviewed. The basis for the volatility representation of the ray diagram is described, with reference to its lack of general applicability to systems in which the total concentrations of solutes in each phase include significant contributions from partitioning of hydrolysis products (i.e., acids and bases) of the original salts. A thermodynamic model based on differing assumed dominant speciation of solutes in liquid and steam is developed and illustrated through application to recent experimental results. The implications of the volatility measurements on solute speciation are outlined through consideration of a fully-speciated thermodynamic model for liquid-vapor equilibria in NaCl(aq). Finally, some future prospects are described for the unambiguous determination of the distribution of solute species in coexisting phases.

EXPERIMENTAL APPARATUS AND TECHNIQUES

Both static and dynamic (flowing) methods have been applied to determine the compositions of

coexisting liquid and vapor phases of aqueous electrolytes at high temperatures. An example of a

quantitative dynamic-sampling method has been described by Goodstine [10]. While this method

has advantages in the possibility of extending the range of measurement to lower liquid-phase

concentrations by collecting and concentrating large samples of equilibrated vapor, the static

method is operationally simpler and has been used in many studies in our laboratories. A

schematic diagram of the apparatus is shown in Figure 1. The stainless steel high-temperature

pressure vessel (HIP Corp.) has an internal volume of approximately 600 cm^3. It contains a close-

fitting platinum-alloy liner of 0.25 mm thickness which is equipped with a platinum alloy

thermowell and sampling lines for both liquid and vapor phases. A third platinum alloy tube is

used to connect the vapor space within the liner to a Teflon bag within a second autoclave at

ambient temperature. The annular space around this Teflon bag is connected in turn to the

annular space in the high-temperature autoclave, and serves to equalize pressure across the liner

through the transport of a small amount of solution. Essentially no fluid is transferred between

the annular space and the liner during equilibration and sampling at constant temperature. A third

autoclave, also at room temperature, contains a chemically-inert syringe (polypropylene and

polyethylene). Samples of the equilibrated vapor phase are obtained by slowly (maximum rate 2

cm$^3 \cdot$h^{-1}) withdrawing water from the annular space of the sampling autoclave into a positive-

displacement pump. Samples of the equilibrated liquid phase are withdrawn directly into an inert

syringe through an inert (PEEK; Upchurch Scientific) valve as shown at the top of Figure 1.

Sample contamination and quantitative trace-level analysis of the vapor phase samples are two primary sources of uncertainty in determining the compositions of coexisting phases. Differences between liquid- and vapor-phase concentrations of low-volatility solutes can be greater than 8 orders of magnitude, depending on temperature and solution concentration. Thus contamination of a vapor sample with as little as 0.01 per cent entrained liquid could give an apparent vapor-phase solute concentration which is higher than the actual concentration by a factor of 10^4. Checks for possible contamination of vapor samples are made through varying the sampling rate and by the use of tracers (e.g., low levels of KCl in NaCl solutions) in the liquid phase. Sample analyses are carried out using a number of techniques as appropriate, with acidimetric titration, standard- or concentrator-mode ion chromatography, and flame-ionization or graphite-furnace atomic absorption spectroscopy used for most samples.

One of our early investigations [11] on the volatility of hydrochloric acid indicated that this acid was much more volatile than chloride salts (e.g., NaCl), and all experiments have included the use of pH control and/or full analyses for both cation and anion concentrations in steam condensate samples to insure that erroneous results did not arise through partitioning of hydrolysis products.

RESULTS AND DATA ANALYSIS

The direct results of sampling and analysis of the compositions of coexisting phases are the molality (or other appropriate composition variable) ratios in the two phases, i.e., m_v/m_l where the subscripts v and l refer to vapor and liquid phases, respectively. Due to the effects of activity coefficients and/or speciation of the solute in the two phases, this ratio is not in general expected

6

to be independent of total solute concentration in either phase. It is instructive here to consider

both the basis for the ray diagram and the assumptions used to develop our more recent

thermodynamic treatment of phase equilibrium results.

Basis of the Ray Diagram

The most common representation of the ray diagram is that given in Figure 2, where the ratio of

concentrations of solute in the two phases is a linear function of the ratio of the densities of the

phases when each is plotted on a logarithmic scale. This relationship must be true near infinite

dilution at the solvent critical point, where the two phases have identical compositions. The steep

negative slope of the individual "rays" in the diagram indicate the strong prograde partitioning of

solutes to steam with increasing temperature for relatively nonvolatile solutes. The opposite is

true for relatively volatile solutes; NH_3 lies above zero at all points on this plot, with positive

slope [12].

The chemical equilibrium between a pure crystalline compound MX and a generalized hydrate

species $MX \cdot nH_2O$ in phase p is given by

$$MX(c) + nH_2O(p) = MX \cdot nH_2O(p) \tag{1}$$
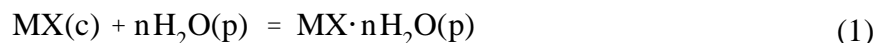
The equilibrium constant for reaction (1) may be written as

$$K_p = \frac{a_{MX \cdot (H_2O)_n}(p)}{a_{H_2O}^n(p)\, a_{MX}(c)} \tag{2}$$

Taking the activity of the crystalline MX equal to unity and substituting liquid (l) and vapor (v) designations for the general phase p gives after some rearrangement

$$\log\frac{a_{MX\cdot(H_2O)_n}(v)}{a_{MX\cdot(H_2O)_n}(l)} = \log\frac{K(v)}{K(l)} - n\log\frac{a_{H_2O}(l)}{a_{H_2O}(v)} \tag{3}$$

The assignment of a single value for n in equations (2) and (3) is an important assumption. This assignment is made based on the assumption that a single hydrate species will predominate in both phases. In principle, this hydration number should be expected to change significantly with temperature and particularly with density. Within this assumption, the quantities $K(v)$ and $K(l)$ are dependent only on temperature and pressure. Along the liquid-vapor critical line for this system the activities of all components in each phase must be equal, and $\{K(v)/K(l)\}_{crit} = 1$. Approximating $K(v) = K(l)$ for $\{T,p\}$ conditions removed from the liquid-vapor critical line gives

$$\log\frac{a_{MX\cdot(H_2O)_n}(v)}{a_{MX\cdot(H_2O)_n}(l)} = -n\log\frac{a_{H_2O}(l)}{a_{H_2O}(v)} \tag{4}$$

Approximating the activities of these components as equal to their concentrations, and assuming that the single hydrate species $MX\cdot(H_2O)_n$ is the predominant solute species in each phase such that its concentration is approximately equal to the total stoichiometric concentration $c(p)$ in each phase gives

$$\log\frac{c(v)}{c(l)} = -n\log\frac{\rho_{H_2O}(l)}{\rho_{H_2O}(v)} \tag{5}$$

8

Equation (5) is the form most generally given for the ray diagram; changing from a molar concentration basis to the molal basis only changes the value of n by 1. The single fitting parameter n is identified as the number of waters of hydration of the solute in each phase. This parameter is positive for relatively nonvolatile compounds, which partition more strongly to the vapor phase with increasing temperature. A negative value for n, implying negative hydration or exclusion of water from the vicinity of a solute molecule, is needed to describe the partitioning of volatile solutes (e.g., ammonia).

A number of relatively severe approximations were used in obtaining equation (5). Styrikovich et al. [13] noted that the distribution ratio $c(v)/c(l)$ will generally not be independent of concentration, and this point will be developed further below. It is more important for practical applications to note that the ray-diagram approach is difficult to apply to general mixed electrolyte and/or concentrated solutions, and that no straightforward accounting for the effects of hydrolysis (e.g., volatility of acids) is incorporated into the treatment. A more flexible general treatment for the distribution of solutes between phases was needed to account for the composition dependence of the distribution ratio and the contributions of hydrolyzed species to the total solute concentration in the vapor phase.

Partitioning Equilibrium Constants

In developing this treatment the extent of ionization of an electrolyte in each phase, rather than the hydration of the solute, is taken as a starting point. The relevant equilibria for ion association and phase partitioning of a simple electrolyte MX are

$$M^+(aq,l) + X^-(aq,l) = MX(aq,l)$$

$$M^+(aq,v) + X^-(aq,v) = MX(aq,v)$$

$$M^+(aq,l) + X^-(aq,l) = M^+(aq,v) + X^-(aq,v)$$

$$MX(aq,l) = MX(aq,v) \tag{6}$$

where due to mass balance only three of these equilibria are independent. The equilibrium

constant for ion association of MX in either phase may then be written as

$$K_A = \frac{m_{MX}(aq)\gamma_{MX}(aq)}{m_M(aq)\gamma_M(aq)\,m_X(aq)\gamma_X(aq)} \tag{7}$$

This equilibrium constant for ion association in the liquid phase may be combined with that for the

partitioning of the neutral species MX between liquid and vapor to give an equilibrium constant

for the distribution reaction

$$K_D = \frac{m_{MX}(aq,v)\gamma_{MX}(aq,v)}{m_M(aq,l)\gamma_M(aq,l)\,m_X(aq,l)\gamma_X(aq,l)} \tag{8}$$

It can be estimated based on electrical conductance measurements [14, 15] that K_A is very large at

the relatively densities characteristic of subcritical steam along the liquid-vapor saturation curve.

Under conditions where the solute is negligibly ionized in steam, the equilibrium constant for the

overall partitioning of MX between liquid water and steam is represented well by equation (8).

Activity coefficients for uncharged solutes in aqueous solutions at low molalities are generally

near unity, except very near the solvent critical point. Adopting this approximation and limiting

consideration to a single solute MX, eq. (8) takes the simple form

$$K_D = \frac{m_v}{m_l^2 \gamma_1^2} \tag{9}$$

where γ_1 is the stoichiometric mean-ionic activity coefficient of MX in the liquid phase.

The distribution constant K_D of equation (9) does not approach unity at the solvent critical point. Combining equations (7) and (8) and noting that the activities of associated MX in the liquid and vapor phases become identical at infinite dilution as the solvent critical point is approached gives the simple relation

$$K_D(T_c, p_c) = K_A(T_c, p_c) \tag{10}$$

Thus for solutes for which K_A has been determined by electrical conductance or other methods at elevated temperatures and fitted such that $K_A(T_c, p_c)$ can be estimated, the value of $K_D(T_c, p_c)$ obtained from fitting volatility results can be compared with an independent value at the critical point, or can be included with values obtained from volatility measurements to give additional data for fitting $K_D(T)$.

Experimental Results and Fitting

Determination of $K_D(T)$ from measured compositions of coexisting phases according to equation (8) or (9) requires values of the activity coefficient of the solute in the liquid phase at the temperature and concentration of the experiment. In principle these values could be determined through simultaneous fitting of the equilibrium constant with parameters of an appropriate model for activity coefficients such as the ion interaction treatment of Pitzer (16). In practice the limited

molality range over which coexisting-phase compositions can be determined reliably makes it more practical to use activity coefficients determined independently over the full temperature range of interest (e.g., refs. (17) and (18)), or estimates based on available values to high temperature coupled with extrapolations based on differences between ln γ for the compound of interest and an appropriate reference compound (12). An exception arises for mixed electrolytes, where information on the effect of mixing on activity coefficients can be obtained from measurements of liquid-vapor equilibria of one or both solutes in the mixture as discussed in further detail below.

A selection of values of $K_D(T)$ obtained from measurements of phase equilibria at ORNL is shown in Figure 3. For relatively nonvolatile electrolytes the strong increase in K_D with increasing temperature is clearly evident. Most of the experimental results can be fitted to nearly the experimental uncertainty with a simple function of temperature and solvent density

$$K_D(T_c, p_c) = a + b/T + c \log \rho \qquad (11)$$

where a, b, and c are adjustable parameters and ρ is the density of liquid water. This expression is a simplification of the equation used by Marshall and Franck (19) to represent the equilibrium constant for the ionization of water, and applied to other ionization reactions by Mesmer et al. (20). Values of the density of water used in this program were calculated at the pure-water saturation vapor pressure from the equation of state of Haar, Gallagher, and Kell (21). Slightly modified or extended forms of equation (11) can be used for experimental results which span a relatively wide temperature range with high precision (11, 12). Conversely, for solutes for which low volatility or thermal instability precludes precise measurements of volatility over wide ranges

of temperature (e.g., refs. (22) and (23)), an "isocoulombic" representation (24) with equivalent charges on both sides of the reaction can be written based on known ionization reaction quantities:

$$H_2O(l) + NH_4^+(aq) + HSO_4^-(aq) = NH_4HSO_4(v) + H^+(aq) + OH^-(aq) \qquad (12)$$

As written in equation (12) the heat capacity change for the partitioning reaction can be approximated as $\Delta C_p^\circ = 0$ and the third term on the right hand side of equation (11) can be neglected.

Volatilities in Mixed Electrolytes

Most systems of practical interest involve multiple solutes in aqueous solution. This is particularly true in natural systems at high temperatures such as geothermal reservoirs. For these systems the effects of one electrolyte component on the volatility of a second solute can be used to model changes in the activity coefficient in the mixed electrolyte. An example is the volatility of HCl in {HCl + NaCl}(aq) mixtures. For this system a consistent treatment of the stoichiometric activity coefficients of the individual pure electrolytes was developed (25) which extends the linear approximation developed by Pitzer and Mayorga (26) to account for the relatively strong ion association of HCl(aq) at high temperature without explicit recognition of solute speciation. This stoichiometric approach was adopted to provide a consistent representation of activity coefficients in the common-ion mixture without the complication of a fully-speciated treatment of the thermodynamics of NaCl(aq). With values for the pure-electrolyte excess thermodynamic properties at the temperature, pressure and ionic strength of the mixture, the ion interaction expression for the activity coefficient of a solute MX in a common-ion

13

mixture is

$$\ln \gamma_{MX} = \ln \gamma_{MX}^* + y\Delta\phi^* + ym_X\left\{\theta_{MN} + m_X\left(1 - \frac{y}{2}\right)\psi_{MNX}\right\}$$ (13)

where the asterisk quantities are those of the pure electrolyte at the ionic strength of the mixture,

$\Delta\phi^* = \phi_{NX}^* - \phi_{MX}^*$, $m_X = m_{NX} + m_{MX}$, $y = m_{NX}/(m_{NX} + m_{MX})$, and θ_{MN} and ψ_{MNX} are adjustable

parameters.

Measurements were made of the partitioning of HCl from brine to steam over {HCl + NaCl}(aq).

Combining equations (8) and (13) gives an expression for the adjustable parameters in terms of

the predicted and observed vapor-phase molality of HCl:

$$m_X[\theta_{H,Na} + m_X(1 - y/2)\psi_{H,Na,Cl}] = \left(\frac{1}{2y}\right)\ln\frac{m_v(calc)}{m_v(obs)} - \Delta\phi^*$$ (14)

It was found that the three-ion interaction parameter $\psi_{H,Na,Cl}$ was not needed to represent the

partitioning results within experimental uncertainty. Values of the parameter $\theta_{H,Na}$ as a function of

temperature obtained from the vapor-liquid equilibrium measurements are compared in Figure 4

with those determined from measurements of the enthalpy of mixing of NaCl with HCl (27). The

consistency between the parameter values from the two sets of experiments is very good.

Fully-speciated Treatment of Volatility Results

Widely differing assumptions concerning the speciation of solutes in liquid water and steam lead

to significant differences between the ray diagram and the thermodynamic equilibrium constant

models in the predicted partitioning behavior of ionizable solutes under conditions where

14

measurements are not practical. For a simple electrolyte MX (e.g., NaCl), if it is assumed that the only species present are ion pairs MX and ions M^+ and X^-, there are four limiting cases involved in the complete description of the partitioning of MX between liquid and vapor. Of these, the assumption that the solute is primarily ionized in liquid water and ion-paired in steam forms the basis for the thermodynamic equilibrium constant treatment of partitioning data discussed in detail above. The reverse limit (paired in liquid, ionized in steam) is unlikely to be realized in aqueous solutions as both the density and dielectric constant of the solvent are higher in liquid water than in steam, promoting ionization of electrolytes in the liquid as compared with the vapor phase at any given (subcritical) temperature and pressure. Under most cases it is not feasible experimentally to extend measurements to conditions where the solute is predominantly ionized in both phases. However, for finite values of the association constants of the solute in both phases, at sufficiently low solute concentrations the solute should dissociate to ions. Under these conditions the fundamental assumption that the solute is predominantly associated in the vapor phase will not be correct, and molality of solute in steam calculated from that model will be lower than the true value for a given liquid-phase composition. In the following section the experimental results for both solute partitioning and speciation are reviewed with emphasis on the available speciation results at high temperatures (t > 350°C). It is under these conditions where the increasing density and dielectric constant of steam promotes the dissociation of solutes to ions.

The problem of determining unambiguously the speciation of even 'simple' electrolytes in solution is difficult to solve by experiment. Spectroscopic techniques (e.g., Raman spectroscopy) have

been used at elevated temperatures to give information on speciation in aqueous solution (28) and on water structure (29). High-temperature neutron-scattering measurements have been made on water (30) and some electrolyte solutions (31). Recent improvements in synchrotron x-ray sources have increased the applicability of EXAFS to determinations of near-ion structural features in aqueous solution, in princple including ion pairing (32, 33). All these techniques are subject to some interpretation, particularly in those cases where one form of solute (ionized or paired) predominates in solution.

Recently significant progress has been made in computer simulations of aqueous solutions using model potentials for water and solutes. For example, Chialvo et al. (34, 35) have calculated ion-association constants for model NaCl(aq) and HCl(aq) at high temperatures and made comparisons of these values with available experimental results. However, the simulation results are not yet sufficiently numerous or reliable to permit their use in calculating solute speciation under the conditions of interest in practical applications.

The best available experimental information on the speciation of electrolytes in high-temperature aqueous solutions has been obtained from measurements of the electrical conductance of dilute solutions over wide ranges of temperature and density. Ho, Palmer, and Mesmer (36) have reported measurements of the conductance of NaCl(aq) from 100 to 600°C at pressures to 3000 bars. Based on their results at temperatures above 350°C, where ion association is experimentally significant, these authors have expressed the equilibrium constant for the ion-association reaction as a function of temperature and solvent density:

$$\log K_A = 0.997 - 650.07/T - (10.420 - 2600.5/T)\log\rho \qquad (15)$$

A density-dependent expression for the partitioning of NaCl(aq) between liquid and steam under the approximations of equation (9) has been given by Simonson et al. (37):

$$\log K_D = -33.31 + 33829/T + 7.152 \log\rho_l + 20.728 \log\rho_v \qquad (16)$$

Similar equations are available for the association constant (15) and distribution constant (11) for HCl(aq). The condition where the molalities of ions and neutral species are equal in the vapor phase can be taken as a limiting condition for the approximation that equation (9) represents the total partitioning between liquid and steam. Ignoring activity coefficients for very dilute solutions and assuming that the density-dependent expressions for ion association can be applied in the low-density vapor phase for which data are not available, the stoichiometric molality m_l^* in the liquid phase corresponding to equivalent ion and neutral-species molalities in the vapor phase is

$$\log m_l^* = 0.5 \log(K_A K_D) \qquad (17)$$

Estimates of m_l^* obtained from equation (17) and the representations for K_A and K_D described above are shown in Figure 5. It is not surprising that HCl, having significant covalent-bonding character, should show smaller m_l^* than NaCl for all temperatures. The calculated values of m_l^* for NaCl are less intuitive, predicting relatively high values for m_l^* which increase with decreasing temperature over the range considered. It must be noted that no effort has been made to reconcile the values of K_A and K_D at (T_c, p_c) where the values calculated from equations (15) and (16) differ by more than an order of magnitude; thus the calculations from equation (17) are approximate at best. Unfortunately these predictions are very difficult to test experimentally. For

example, at 350°C combining log $m_l^* \approx -3$ with log $K_D \approx -1$ gives $m_v^* \approx -7$, which is near the

concentration limit accessible with the most sensitive conductance apparatus currently available

(38).

The analysis above was based on assumed continuity in the density dependence of the association

constant for these solutes across the subcritical vapor-liquid phase boundary. Very different

predictions can be obtained from an extrapolation of the analysis of ionization of NaCl in

supercritical steam determined from mass spectrometric measurements as presented by Pitzer

(39). In that analysis the ionization constants at 400°C for NaCl at steam-like densities ($\rho < 0.1$

$g \cdot cm^3$) were calculated to be more than 10 orders of magnitude smaller than those obtained from

linear extrapolation of the results at liquid-like densities ($\rho > 0.3$ $g \cdot cm^3$), and discontinuities were

predicted for the density dependence of the ionization constant in liquid and vapor phases at

subcritical temperatures. Further theoretical and experimental investigations of NaCl(aq)

ionization in steam at high subcritical temperatures are needed to improve quantitatively the

representation of NaCl volatility given in equation (16).

A final point is important to the consideration of solute speciation and its effect on the calculation

of liquid-vapor partitioning of solutes over wide ranges of temperature and solution composition.

As has been shown in experimental studies on the volatility of NH_4Cl (12), the partitioning of

conjugate acids (e.g., HCl) is often the dominant contribution to the total anion molality in steam.

These acids are generally ion-paired to a much stronger degree than are the salts. The ratio of

acid volatility to salt volatility at high temperatures is important to the calculation of pH in liquids

18

formed as steam condensate at lower temperatures. However, in these more concentrated

condensates it seems clear that the partitioning of solutes from steam to condensate will best be

described in terms of neutral solutes in steam in equilibrium with predominantly ionized solutes in

the coexisting liquid.

SUMMARY AND CONCLUSIONS

A principal application of the results of measurements and modeling of the partitioning of solutes

between liquid water and steam is the prediction of the composition of coexisting phases at

various points in the steam cycles used in power generation (e.g., fossil, nuclear, or geothermal).

In general, nonvolatile solutes will partition very strongly to the "early condensate" liquids formed

on partial condensation of steam at temperatures significantly below the original steam-formation

temperature. This behavior, which is driven by the strong prograde temperature dependence of

salt volatility, leads to the formation of relatively small amounts of condensate with solute

concentrations many orders of magnitude greater than the original boiling liquid, and can result in

serious problems of solid deposition and/or corrosion in operating systems. Detailed calculations

appropriate for various steam cycles have been presented based on the partitioning results and

models described here (23).

Finally, it should be noted that the representations discussed here are inapplicable to the

interesting problem of calculating the compositions of coexisting fluid phases in concentrated

electrolyte solutions above the critical temperature of water. For these conditions appropriate

methods based on equations of state (40) or corresponding-states models (41) are needed to

reflect that the liquid-vapor critical curve for electrolyte solutions at finite concentrations extend to temperatures well above the solvent critical point.

ACKNOWLEDGEMENT

REFERENCES

1. F. G. Straub, "Steam Turbine Blade Deposits," Univ. of Illinois Bulletin v. 43, no. 59, June 1, 1946.

2. M. A. Styrikovich, I. Kh. Khaybullin and D. G. Tskhvirashvili, <u>Doklady Akademii nauk SSSR</u>, 100, No. 6, 1955, pp.1123-1126.

3. M. A. Styrikovich, O. I. Martynova and Z. S. Belova, Doklady Akademii Nauk SSSR, v. 162, no. 4, 1965, 806-809.

4. Y. F. Samoilov and O. K. Smirhov, Teploenergetica, No. 2, 1959, 53-56.

5. M. A. Styrikovich and O. I. Martynova, Soviet Atomic Energy, v. 15, 1963, 917-921.

6. O. I. Martynova, Russ. J. Phys. Chem. 38, No. 5, 1964, pp. 597-592.

7. B. P. Tatarinov, Y. M. Lukashov and A. T. Sholichev, Teploenergetica, v. 13, no. 11, 1966, 59-60.

8.   M. A. Styrikovich, K. J. Katkovskya and I. J. Dubrovski, "The investigation of distribution of sodium hydroxide between water and its steam at high parameters", Collection of Works of the Moscow Power Institute, v. 238, 1975.

9.   O. Jonas, "Transport of Ionic-Impurities in Fossil and PWR Cycles - New Observations". Int. Water Conference, Vol. 42, 1981, No. IWC-81-40.

10.   S. L. Goodstine, "Vaporous carryover of sodium salts in high-pressure steam", Proceedings of the American Power Conference, v. 36, 1974, 784-789.

11.   J. M. Simonson and D. A. Palmer, *Geochim. Cosmochim. Acta* 1993, **57**, 1-7.

12.   D. A. Palmer and J. M. Simonson, *J. Chem. Eng. Data* 1993, **38**, 465-474.

13.   M. A. Styrikhovich, O. I. Martynova, and Z. S. Belova, *Teploenergetika* 1965, 12, 86-89.

14.   A. S. Quist and W. L. Marshall, *J. Phys. Chem.* 1968, **72**, 684-703.

15.   J. D. Frantz and W. L. Marshall, *Am. J. Sci.* 1984, **284**, 651-667.

16.   K. S. Pitzer, *J. Phys. Chem.* 1973, **77**, 268-277.

17.   R. H. Busey, H. F. Holmes, and R. E. Mesmer, *J. Chem. Thermodynamics* 1984, **16**, 343-372.

18.   J. M. Simonson, H. F. Holmes, R. H. Busey, R. E. Mesmer, D. G. Archer, and R. H. Wood, *J. Phys. Chem*. 1990, **94**, 7675-7681.

19.   W. L. Marshall and E. U. Franck, *J. Phys. Chem. Ref. Data* 1981, **10**, 295-304.

20.   R. E. Mesmer, W. L. Marshall, D. A. Palmer, J. M. Simonson, and H. F. Holmes, *J. Solution Chem.* 1988, **17**, 699-718.

21.   L. Haar, J. S. Gallagher and G. S. Kell, NBS/NRC Steam Tables. Thermodynamic and Transport Porperties and Computer Programs for Vapor and Liquid States of Water in SI

Units. Hemisphere Publishing Corporation, New York: 1984.

22.   D. A. Palmer, J. M. Simonson, R. W. Carter, J. P. Jensen, and S. L. Marshall, *Vapor-Liquid Partitioning of Sulfuric Acid and Ammonium Sulfate*, EPRI, Palo Alto, CA: 1999. TR-112359.

23.   D. A. Palmer, J. M. Simonson, R. W. Carter, J. P. Jensen, D. B. Joyce, and S. L. Marshall, *Volatility of Aqueous Sodium Hydroxide, Bisulfate and Sulfate*, EPRI, Palo Alto, CA: 1999. TR-015801.

24.   W. T. Lindsay, Jr., "Estimation of Concentration Quotients for Ionic Equilibria in High Temperature Water: The Model Substance Approach," *Proceedings: 41st International Water Conference*, Pittsburgh, 1980, pp. 284-294.

25.   J. M. Simonson, D. A. Palmer, and S. L. Marshall, "Liquid-vapor phase equilibria of HCl and excess thermodynamic properties of {HCl + NaCl}(aq) mixtures at high temperatures," In *Steam, Water, and Hydrothermal Systems: Physics and Chemistry Meeting the Needs of Industry* (Proceedings of the 13th ICPWS, Toronto, Ontario). P. G. Hill, P. Tremaine, D. Irish, P.V. Balakrishnan, eds. NRC Press, 2000, in press.

26.   K. S. Pitzer and G. Mayorga, *J. Solution Chem.* 1974, **3**, 539-546.

27.   G. H. Zimmerman and J. M. Simonson, unpublished results.

28.   B. S. W. Dawson, D. E. Irish, and G. E. Toogood, *J. Phys. Chem.* 1986, **90**, 334-341.

29.   W. Kohl, H. A. Lindner, and E. U. Franck, *Ber. Bunsenges. Phys. Chem.* 1991, **95**, 1586-1593.

30.   P. Postorino, R. H. Tromp, M.-A. Ricci, A. K. Soper, and G. W. Neilson, Nature 1993, **366**, 668-670.

31.   P. H. K. de Jong and G. W. Neilson, *J. Phys.: Condens. Matter* 1996, **8**, 9275-9279.

32.   J. L. Fulton, D. M. Pfund, S. L. Wallen, M. Newville, E. A. Stern, and Y. Ma, *J. Chem. Phys.* 1996, **105**, 2161-2166.

33.   J. F. W. Mosselmans, P. F. Schofield, J. M. Charnock, C. D. Garner, R. A. D. Pattrick, and D. J. Vaughan, *Chem. Geo.* 1996, **127**, 339-350.

34.   A. A. Chialvo, P. T. Cummings, J. M. Simonson, and R. E. Mesmer, *J. Chem. Phys.* 1996, **105**, 9248-9257.

35.   A. A. Chialvo, P. T. Cummings, and J. M. Simonson, *J. Chem. Phys.*, submitted for publication.

36.   P. C. Ho, D. A. Palmer, and R. E. Mesmer, *J. Solution Chem.* 1994, **23**, 997-1018.

37.   J. M. Simonson, D. A. Palmer and R. W. Carter, "Liquid-vapor partitioning of NaCl(aq) from concentrated brines at temperatures to 350°C," *Proceedings: Stanford Geothermal Reservoir Engineering Workshop,* 1994, **19**, 245-251.

38.   M. S. Gruszkiewicz and R. H. Wood, *J. Phys. Chem. B* 1997, **101**, 6549-6559.

39.   K. S. Pitzer, "Thermodynamics of sodium chloride in steam", J. Phys. Chem., 87, 1983, 1120-1125.

40.   A. Anderko and K. S. Pitzer, *Geochim. Cosmochim. Acta* 1993, **57**, 1657-1680.

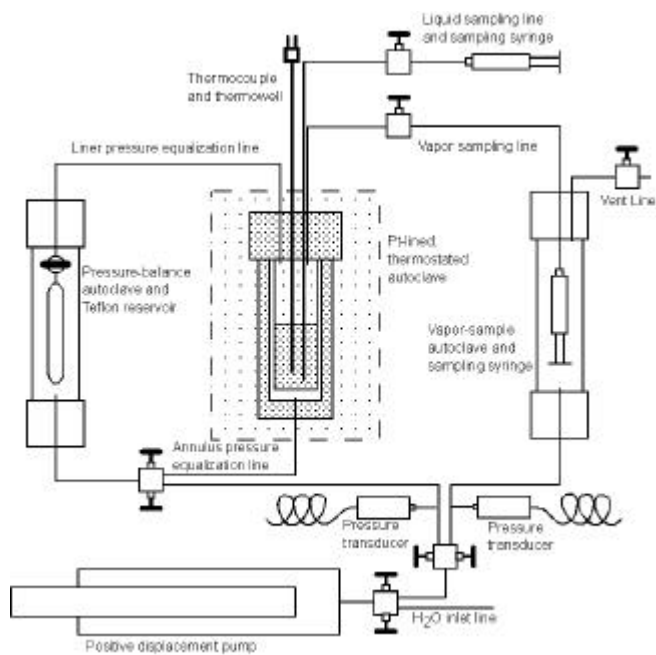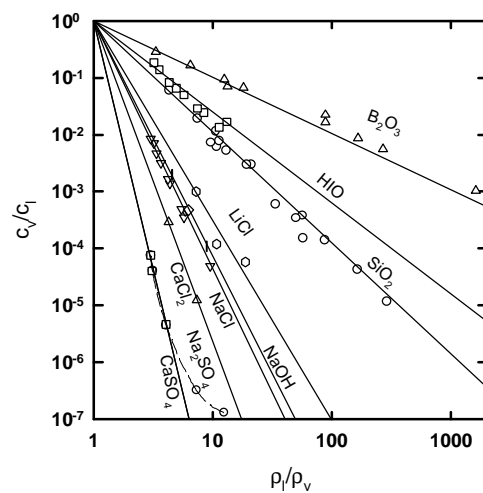41.   J. S. Gallagher and J. M. H. Levelt Sengers, Int. J. Thermophys. 1988, 9, 649-661.
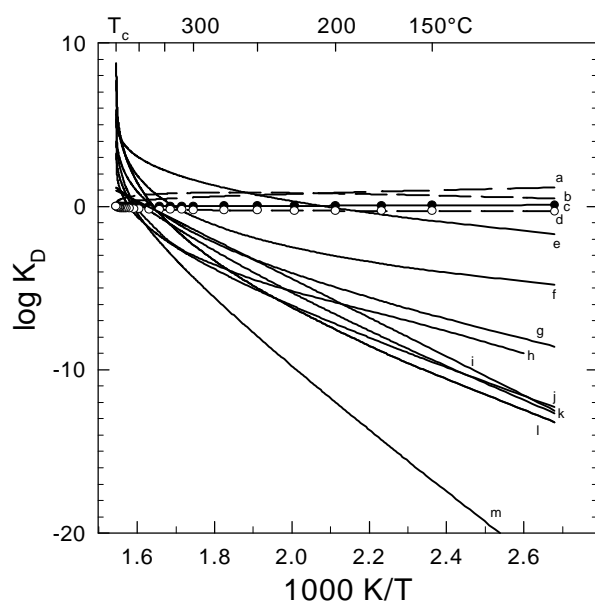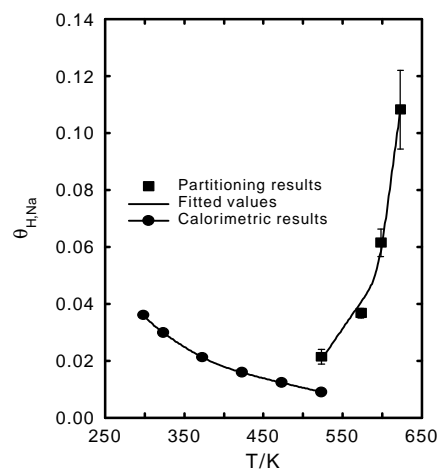
Figure 1.

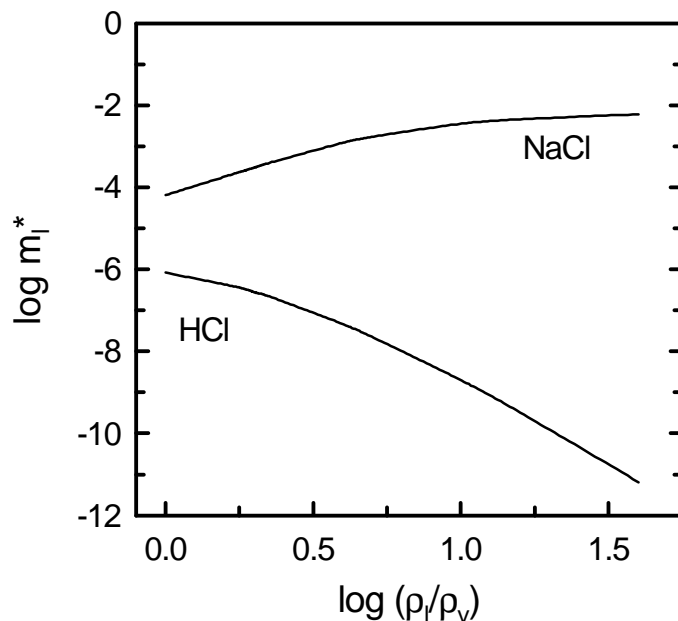
Figure 2.

Figure 3.

Figure 4.

Figure 5.

FIGURE CAPTIONS

Figure 1. Schematic diagram of the static volatility apparatus used in ORNL studies of solute volatility.

Figure 2. A representation of the ray diagram, showing the relationship between solute distribution ratios and the ratio of the densities of liquid water and steam.

Figure 3. Equilibrium partitioning constants $K_D(T)$ determined from ORNL volatility measurements (except NH_3). a, NH_3; b, SO_2; c, Ch_3COOH, d, $HCOOH$; e, HCl; f, NH_4Cl; g, H_2SO_4; h, $NaCl$; i, CH_3COONa; j, $NaOH$; k, NH_4HSO_4; l, Na_2SO_4; m, $NaHSO_4$.

Figure 4. Comparison of the mixed-electrolyte ion-interaction parameter $\theta_{H,Na}$ determined from calorimetric and volatility measurements.

Figure 5. Calculated values of the liquid-phase molality m_l^* corresponding to predicted equivalent molalities of neutral and ionized solute species in steam.